Advances in Industrial and Manufacturing Engineering 8 (2024) 100139

Contents lists available at ScienceDirect

Advances in Industrial and Manufacturing Engineering

journal homepage: www.sciencedirect.com/journal/advances-in-industrial-and-manufacturing-engineering

Influence of changing loading directions on damage in sheet metal forming

Philipp Lennemann *, Yannis P. Korkolis, A. Erman Tekkaya

Institute of Forming Technology and Lightweight Components (IUL), TU Dortmund University, 44227, Dortmund, Germany

ARTICLE INFO

Keywords:
Damage
Sheet forming
Strain path changes
Characterization
Anisotropy

ABSTRACT

The impact of the stress state on damage evolution, fracture behavior, and product performance is well understood for proportional loading. However, many complex sheet forming operations involve non-proportional loading, which affect the material's hardening and fracture characteristics. This study investigates the influence of a loading direction change on damage evolution in a dual phase steel DP800. Specimens are pre-strained by tensile tests and subsequently loaded in either the same or orthogonal direction to the initial pre-strain direction by additional tensile tests and bending tests. Damage quantification by scanning electron microscopy reveals lower damage evolution after an orthogonal change of loading direction in contrast to monotonic loading directions. The load paths, defined as a history of triaxiality and Lode parameter during loading, are identified numerically under consideration of kinematic hardening. Since kinematic hardening leads to higher triaxialities after orthogonal changes, the load path is not the dominant influence on damage. A possible explanation for the experimental results is the void characteristics after tensile load. After the pre-straining in tensile test, voids are oriented orthogonally to the tensile direction and located between hard martensitic phases. The influence of this morphology on subsequent void growth is illustrated by a simulation verifying that an orthogonal change of loading direction results in void shrinkage, while monotonic loading directions lead to further void growth.

1. Introduction

Dual phase steels that consist of martensite and ferrite phases, such as DP800, are widely used in automotive industry due to their excellent combination of high strength and good formability. The microstructure of DP800 is set during the hot and cold rolling processes and intercritical annealing, which can lead to anisotropic ductile behavior. The influence of monotonic stress states during forming on the damage evolution, fracture strains and the performance of parts are frequently investigated. In complex manufacturing sequences, but also in simple processes such as deep drawing, individual sheet metal regions undergo various stress states with changes regarding the hydrostatic and deviatoric stress state. One aspect of these non-proportional load paths is the change of the direction of the mean stress. Therefore, this study aims to investigate the influence of a change of loading direction on the development of damage, while separating the effects of the stress state and the rolling induced microstructure.

Damage is the nucleation, growth and coalescence of voids. Damage mechanisms depend on the material. Voids nucleate by fracture of phases and non-metallic inclusions or decohesion of two phases or between a phase and an inclusion. The main damage mechanisms in dual phase steels are martensite cracking and interfacial decohesion at martensite/ferrite interfaces (He et al., 1984). These voids are oriented orthogonal to the loading direction in tensile tests at small strains and then grow along the loading direction (Ahmad et al., 2000).

Direct methods for the characterization of damage evolution are based on density measurements and 2D microscopic images. Density measurements are also influenced by the dislocations, which have to be considered during the evaluation of damage. Microscopic measurements on the other hand are influenced by the preparation process of the specimen.

Before annealing, the microstructure of dual phase steels consist of pearlite colonies and elongated ferrite grains due to cold rolling, which define the morphology of the final ferrite-martensite structure (Avramovic-Cingara et al., 2009). Investigations on DP800 steels showed that martensite morphology and distribution have a significant influence on the accumulation of damage and fracture (Avramovic-Cingara et al., 2009). Niazi et al. (2013) have shown, that a DP600 grade is showing anisotropic behavior in the post necking localization regarding damage evolution and fracture when loaded in and transverse to the rolling direction albeit showing isotropic behavior up to necking. This is attributed to the anisotropy of martensite morphology.

* Corresponding author.
E-mail address: Philipp.Lennemann@iul.tu-dortmund.de (P. Lennemann).

https://doi.org/10.1016/j.aime.2024.100139
Received 5 December 2023; Received in revised form 26 February 2024; Accepted 5 March 2024
Available online 12 March 2024

Besides the choice of material, damage evolution is influenced by the stress state during forming (i.e., the load path). For the description of the load path and its influence on damage and failure, the Lode parameter L and the stress triaxiality η are frequently used. While the triaxiality influences growth, or if negative, even shrinking of already nucleated voids in the microstructure (McClintock, 1968), the Lode parameter influences the evolution of the void's shape (Barsoum and Faleskog, 2007). The stress triaxiality η is given by

$$\eta = \frac{\sigma_h}{\sigma_{vM}}, \tag{1}$$

with the hydrostatic stress σ_h and the von Mises equivalent stress σ_{vM}.

Former investigations in air bending have shown that compressive stresses introduced in the forming zone at the outer fiber, lower the hydrostatic stresses (i.e., the triaxiality), hence, reducing damage (void area fraction) and increasing the parts performance such as fatigue strength, impact strength and elastic stiffness (Meya et al., 2019).

The deviatoric stress state can be described by the Lode parameter L (Lode, 1926), which is the position of the second principal stress relative to the first and third principal stress:

$$L = \frac{2 \bullet \sigma_2 - \sigma_1 - \sigma_3}{\sigma_1 - \sigma_3}. \tag{2}$$

with the principal stresses σ_1, σ_2 and σ_3.

Although the Lode parameter does not influence the size of voids but rather their shape, it still influences the fracture strains. The triaxiality and Lode parameter are frequently used in damage models to predict fracture. High triaxialities as well as a Lode parameter in the region of shear loading at $L = 0$ leads to low fracture strains (Bai and Wierzbicki, 2008). As shown by Wierzbicki and Xue (2005), the Lode parameter can be derived from the triaxiality for plane stress conditions, which appear in most sheet metal forming operations.

In multistep metal forming processes, the material might experience non-constant load paths regarding the triaxiality and Lode parameter, which can be considered as load path changes. However, both triaxiality and Lode parameter represent the stress state in a reduced form, because the spatial orientation of the mean stresses is not considered, which is important for effects like anisotropic hardening.

For the classification of two subsequent and discrete load steps, Schmitt et al. (1985) proposed to use a parameter, which refers to both a change of deviatoric stress state as well as a change regarding the spatial orientation:

$$\kappa = \frac{\Delta\varepsilon_1^{pl} : \Delta\varepsilon_2^{pl}}{\left\|\Delta\varepsilon_1^{pl}\right\| \bullet \left\|\Delta\varepsilon_2^{pl}\right\|} \tag{3}$$

where $\Delta\varepsilon_i^{pl}$ is the tensor corresponding to the plastic strain increment of load step i.

The parameter κ can vary between $-1 < \kappa < 1$ and represents following strain paths.

- $\kappa = 1$: monotonic strain path
- $1 < \kappa < 0$: monotonic strain path change
- $\kappa = 0$: orthogonal strain path change
- $0 < \kappa < -1$: non-monotonic strain path change
- $\kappa = -1$: strain path reversal

A change of loading direction influences hardening. Anisotropic hardening is commonly known and leads generally to lower flow stresses after a strain path change (Bauschinger, 1886). Besides the Bauschinger effect, transient hardening, work-hardening stagnation, and permanent softening are observed. The cross-hardening effect describes an increase in flow stress after orthogonal strain path changes. Isotropic hardening assumes that hardening evolves equal in all directions by expansion of the yield surface. The relation between equivalent plastic strain and flow stress is defined by experimental flow curves or mathematical functions, e.g. Ludwik (1909), Voce (1956). The first kinematic hardening model was introduced by Prager (1945) and later enhanced by Ziegler (1959). Kinematic hardening models assume a translation of the yield surface, while the shape is not altered. Multiple models can capture mixed isotropic and kinematic hardening, such as Chaboche (1986), HAH (Barlat et al., 2011) or Yoshida and Uemori (2002). For dual phase steels, Tarigopula et al. (2008) investigated the hardening behavior of sheet material after changing the loading direction. Their results of pre-strained tensile specimen show a reduction in initial flow stress after conducting a second tensile test orthogonal to the initial direction. The material exhibits a fading memory of the change of loading direction with subsequent plastic straining, which may indicate that residual phase stresses lead to the transient anisotropic behavior. Ha et al. (2014) investigated experimental and numerical responses of dual phase steels after an orthogonal change of loading direction. Analyses using representative volume elements were conducted with a cross-hardening response for ferrite phase. Results have shown, that an increase of martensitic volume fractions (10 % and 30 %) leads to attenuation of the cross-hardening effect. The softening response was analytically explained using one-dimensional analysis of a tension-compression sequence. The application of the Chaboche model for dual phase steel has shown very good agreement for the anisotropic behavior in uniaxial tension-compression experiments (Deng et al., 2018).

Investigations on strain path changes have shown, that non-proportional strain paths lead to higher fracture strains than proportional strain paths. However, these results show the mixed effect of non-proportional hydrostatic and deviatoric stress states as well as a changing spatial orientation of the loads. To address the effect of non-proportional load paths on fracture, Sampaio et al. (2023) have evaluated the stress state in an average sense for the whole forming process. Kestner and Koss (1987) have conducted combinations of uniaxial and equibiaxial tension on titanium sheet which leads to a final state of plane-strain. The non-proportional strain paths lead to higher fracture strains compared to proportional strain paths. As a contributing factor, they cited the delay of void nucleation during multi-stage straining using strain paths that are characterized by small maximum principal stresses.

The analysis of the literature reveals that the influence of varying loading directions on hardening has been thoroughly investigated and modelled. Strain path changes show an effect on fracture, while the reasons are not understood and damage has not been investigated yet. Current damage models depend on Lode parameter and triaxiality to predict damage evolution, while changes of the loading direction are usually not included. The void morphology in dual phase steel depends on the direction of mean stress in uniaxial tensile load. This can lead to load direction dependent damage evolution. Since the microstructure and therefore the mechanical properties are influenced by the rolling process and the annealing process, the loading direction w.r.t. the rolling direction has an influence on damage and fracture.

This paper aims to investigate the influence of changes regarding the loading direction in tensile-tensile and tensile-bending sequences on damage evolution in a dual phase steel DP800. To show the isolated influence of changes regarding the loading direction on damage evolution, the stress state as well as the rolling induced microstructure needs to be taken into account. The influence of the stress state is identified by triaxiality and Lode parameter. The influence of the load direction w.r.t. the rolling direction is assessed by taking the orientation of tensile and bending stresses into account.

First, the influence of changing load directions on damage evolution is investigated for tensile-tensile sequences by the determination of void area fractions. The specimens are loaded in the same direction as the pre-strain and the orthogonal direction to the pre-strain (Section 2). To exclude the effect of rolling-induced anisotropy of the sheet material, specimens for pre-straining the material are extracted in diagonal direction (DD). This results also in diagonal directions for the second tensile test in monotonic as well after an orthogonal change of the load

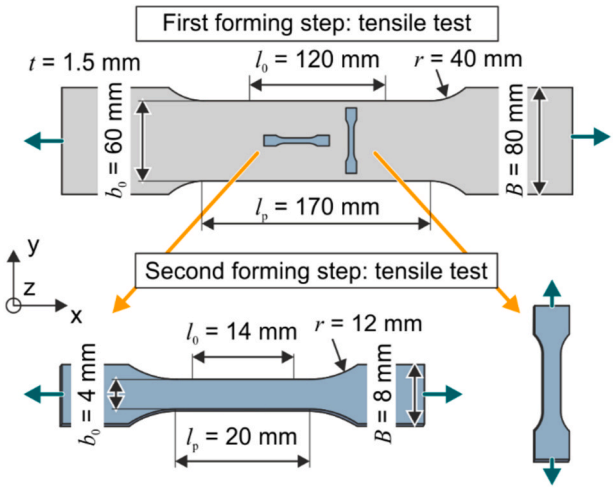

Fig. 1. Geometries of specimens for tensile-tensile sequences.

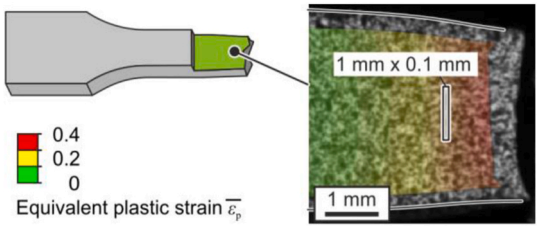

Fig. 2. Area for damage characterization via SEM on necking area of tensile specimen with the strain distribution of the subsequent tensile test.

direction. To assess the impact of damage evolution on failure the fracture strains are determined. In the next step (Section 3), the influence of the void morphology after tensile tests on the further void growth is illustrated by a simulation where uni- and cross-directional load conditions are applied on the already nucleated voids.

To investigate a complex process chain, the damage evolution in tensile-bending sequences is investigated for specimen that are loaded in the same and in the orthogonal direction to the pre-strain (Section 4). This leads to a non-monotonic load path due to a change from uniaxial tension to plane strain condition in bending. As in the tensile-tensile sequences, loads in diagonal direction are used to separate the effect of anisotropic behavior due to the prior rolling process. Regarding the subsequent bending test, the plane strain condition with the assumption of isotropic hardening leads to a triaxiality of 0.58 and a Lode parameter of zero on the outer fiber. To consider anisotropic hardening, the stress state during the bending test is determined by a simulation with anisotropic hardening model by Chaboche. The parameters for the model are assessed by the flow curves of the tensile-tensile test sequences. The influence of the previous rolling process on damage evolution is regarded by additional tests in rolling direction and transverse direction (RD, TD).

2. Damage evolution in tensile-tensile sequences with changing loading directions

To investigate the effect of a load direction change, while keeping triaxiality and Lode parameter constant, tensile-tensile tests were conducted (Fig. 1). Large tensile tests with a testing area of 120 × 60 mm were conducted in the first forming step, and were stopped briefly before necking occurs to obtain homogenously pre-strained specimen, that allow extraction of smaller specimen for a subsequent tensile test. Since necking sets in at an equivalent plastic strain of 0.105, the pre-strain was chosen to be 0.09. Strains were measured using a tactile extensometer with an initial gauge length of 120 mm. The testing area of the subsequent tensile specimen was 14 × 4 mm. The testing speed is 0.0067 1/s for a parallel length of 18 mm. Aramis DIC was used to measure the apparent maximum strain according to von Mises strain before fracture. The rate is 5 frames/s and the reference length is 0.6 mm.

Uniaxial tension leads to a triaxiality of 0.33, and a Lode Parameter of −1. The Schmitt parameter κ is calculated to classify the occurring strain path changes. Therefore, the strain vectors of the pre-straining and the subsequent tensile tests are defined for the coordinates x, y and z according to Fig. 1. Assuming isotropic plastic behavior, the following strain vector is present in the pre-straining tensile test:

$$d\vec{\varepsilon}_p^{1} = \begin{pmatrix} d\varepsilon_p^x \\ d\varepsilon_p^y \\ d\varepsilon_p^z \end{pmatrix} = \begin{pmatrix} d\varepsilon_p^x \\ -d\varepsilon_p^x/2 \\ -d\varepsilon_p^x/2 \end{pmatrix} \tag{4}$$

When loaded in the same direction as the pre-straining tensile test, the strain vector of the subsequent tensile test $d\vec{\varepsilon}_p^{2,uni}$ is equal to $d\vec{\varepsilon}_p^{1}$, which, according to Eq. (3), leads to a monotonic strain path ($\kappa = 1$).

When loaded cross directional to the pre-straining tensile test, the strain vector of the subsequent tensile test is

$$d\overrightarrow{\varepsilon_p^{2,cross}} = \begin{pmatrix} d\varepsilon_p^x \\ d\varepsilon_p^y \\ d\varepsilon_p^z \end{pmatrix} = \begin{pmatrix} -d\varepsilon_p^y/2 \\ d\varepsilon_p^y \\ -d\varepsilon_p^y/2 \end{pmatrix} \tag{5}$$

This orthogonal change of loading direction leads to a non-monotonic strain path change with $\kappa = -0.5$.

Damage evolution can be quantified by the void area fraction D_s in microscopic observations (Lemaitre and Dufailly, 1987):

$$D_s = \frac{S_D}{S} \tag{6}$$

with the void area S_D and the investigated area S.

The void area fractions are evaluated in the necking area along the thickness direction of the sheet (Fig. 2) at a plastic equivalent strain of 0.35 (pre-strain + strain in subsequent tensile test: 0.09 + 0.26). This strain was chosen by the comparison of the necking area of all specimen with the aim, that the geometry regarding the thickness and width and therefore the strains are equal for all specimen up to this region. Since this region has a heterogeneous strain distribution, damage is characterized by SEM-imaging. The view in thickness direction enables an orthogonal sight on the damaged area in regards of the applied loads in both sequences. To prepare the samples, a water-cooled cutting machine is used to section them out from the specimens, which are then embedded with a hot mounting press. The sample preparation process involves mechanical grinding and polishing. The first grinding step removes 0.75 mm of the sample using 80 µm sandpaper to access the central area of the sheet thickness. The samples are subsequently etched with Nital-3% for 2–3 s. To acquire 2D images, a scanning electron microscope (Tescan MIRA III XMU) equipped with a secondary electron detector at a cathode voltage of 15 kV is used. Greyscale matching is used to determine the void area fraction. 10 images covering an area of 100 × 100 µm each are captured over an area of 1 mm in a defined region with an equivalent plastic strain of 0.35.

Specimens with a constant loading direction ($\kappa = 1$) exhibit a larger void area fraction than specimen after an orthogonal change of loading direction ($\kappa = -0.5$) (Fig. 3a). The factor is between three to four times. This, in turn, is beneficial for the fracture strain, which increases about 15 % with lower void area fraction (Fig. 3b). Although the specimens are subjected to the same stress state during forming (load path), damage evolution and fracture strains differ. A possible reason for this is the void morphology after uniaxial tensile load. This hypothesis is shown in the following section.

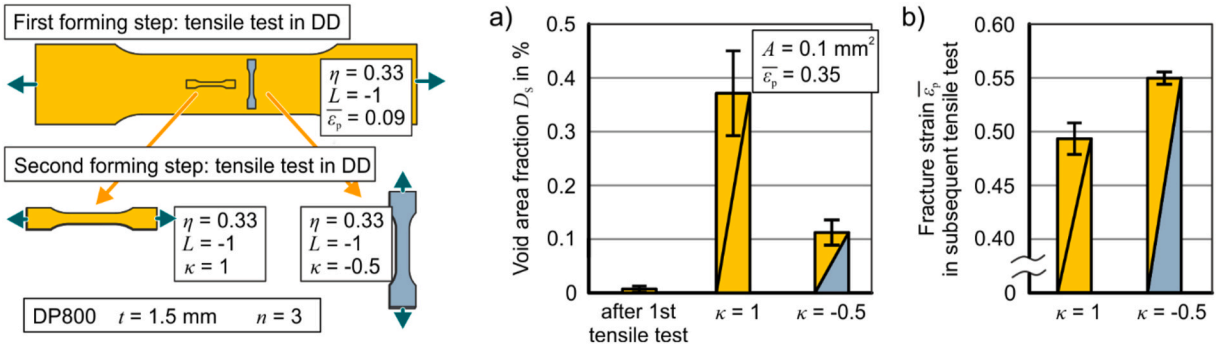

Fig. 3. Tensile-tensile sequence: a) Void area fraction in tensile specimen after pre-strain and after subsequent uniaxial and cross loading and b) Fracture strain in second stage tensile test with and without a change of loading direction.

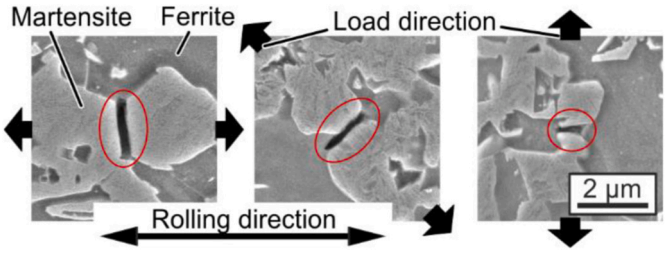

Fig. 4. Damage in tensile specimen at a strain of $\varepsilon_p = 0.09$ in RD, DD, TD specimen.

3. Influence of void morphology on further void growth

Damage evolution was investigated for the pre-strained specimen. The voids that were found are positioned between two martensite islands in the majority of cases (Fig. 4). The underlying mechanism could be a martensitic fracture or a ferritic failure between two martensitic islands. The orientation of the voids is predominantly transverse to the direction of loading regardless of the rolling direction. Therefore, the void orientation and its position between martensitic islands is only dependent on the loading direction. Regarding the pre-straining tensile tests, the voids are therefore surrounded by hard martensite phases in pre-strain direction and by softer ferrite phases in the orthogonal direction. It is hypothesized that this formation plays an important role in the following forming steps, since an orthogonal change of loading direction could lead to different growth of those already nucleated voids compared to specimen that have a monotonic loading direction.

An illustrative simulation is set up to show the influence of this formation due to the differences in hardening of ferrite and martensite phases. The simulation depicts two martensitic phases in a ferrite matrix with a void in between that is oriented orthogonal to the supposed first tensile load (Fig. 5a). The model is setup in Abaqus (2019) with an implicit solver. The martensitic phase comprises an area fraction of 20% (Pütz et al., 2020). The element type is CPS4R (plane stress, 4-node bilinear, reduced integration with hourglass control). The whole model consists 12,800 elements. The load is applied by a displacement for a global strain of 0.05. Both martensitic and ferritic phases are modelled with isotropic hardening with flow curves from Ramazani et al. (2013).

After monotonic loading the void increases in size, while after an orthogonal change of loading direction the void area shrinks (Fig. 5b). This leads to the expectation of lower void area fractions after cross directional loading in tensile tests in comparison to the uni-directionally loaded specimen which fits the experimental results (Fig. 3a).

4. Damage evolution in tensile-bending sequences with changing loading directions

4.1. Experimental determination of damage evolution

The tensile-tensile sequences enabled an isolated view on load direction changes, while keeping the load path constant. In regards of complex sheet metal forming processes, tensile-bending sequences are investigated, where not only the load direction is changed, but also the hydrostatic and deviatoric stress state. Therefore, bending tests are conducted, where the bending stresses are aligned and orthogonal to the tensile pre-strain direction (Fig. 6a). For each loading direction w.r.t. the rolling direction, three tensile specimens were pre-strained as described

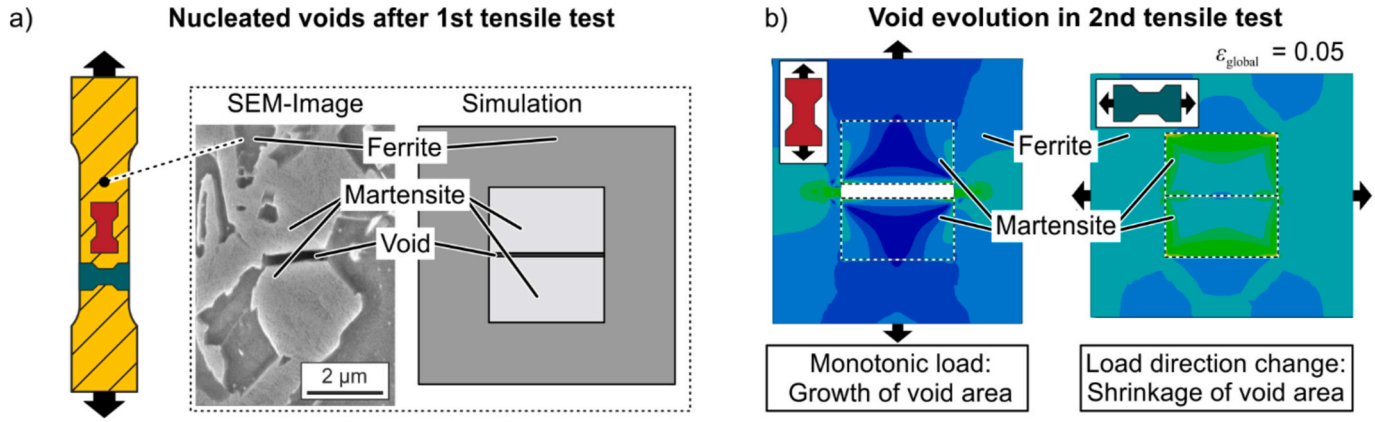

Fig. 5. a) Position of voids in between two martensitic phases after pre-strain and its illustration in a simulation and b) Simulation of void evolution in subsequent tests at monotonic loading and after orthogonal change of loading direction.

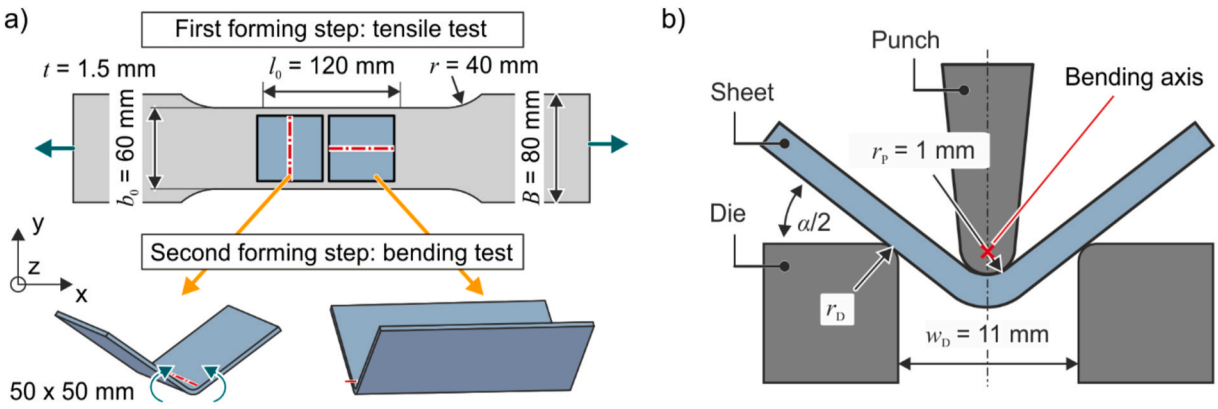

Fig. 6. a) Geometries of specimens for tensile-bending sequences and b) Air bending test setup.

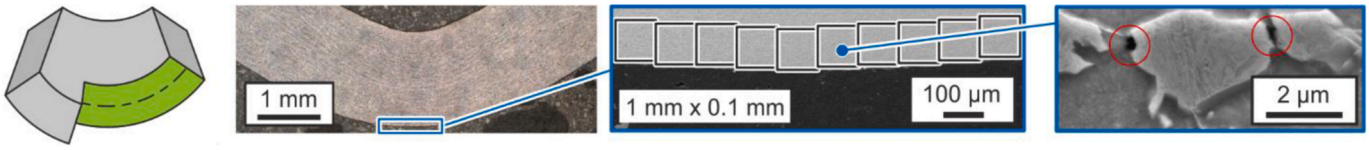

Fig. 7. Area for damage characterization via SEM on the outer fiber of bending specimen.

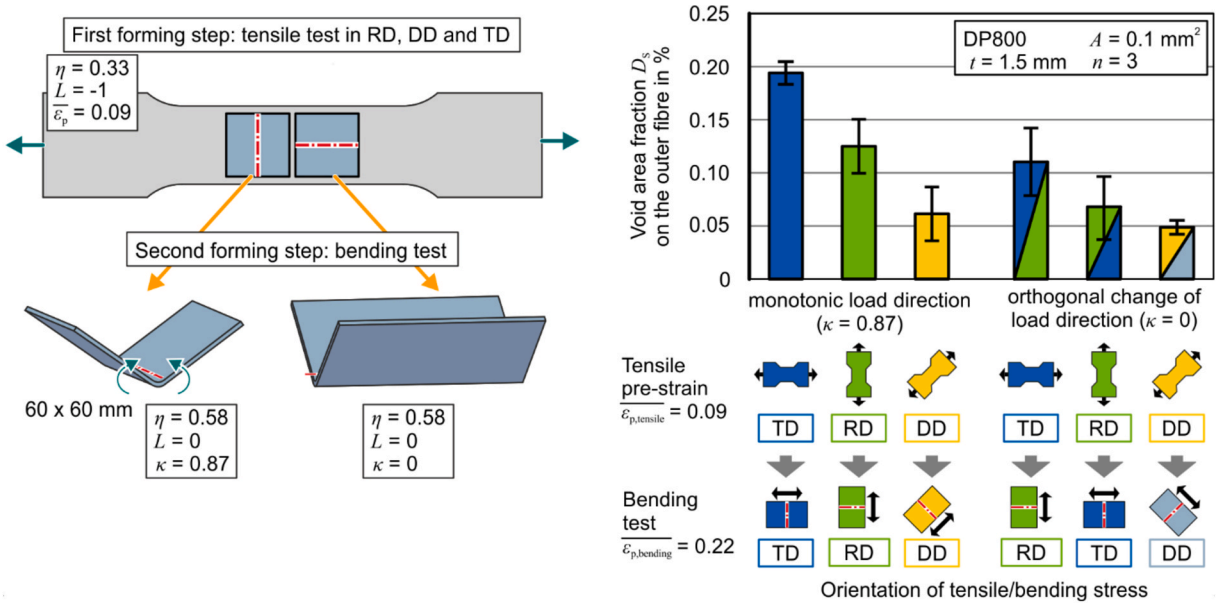

Fig. 8. Tensile-bending sequence: Void area fraction after subsequent bending test in rolling direction (RD), diagonal direction (DD) and transverse direction (TD).

in section 2. In the second forming step bending tests were performed. Two bending specimens were cut out of each specimen, from which one was bent in parallel and one was bent in orthogonal direction. The dimensions of the bending specimen are 50 × 50 mm. The tests were conducted at a Trumpf TrumaBend V1300X bending machine. The punch radius for the bending tests is 1 mm, die width is 11 mm and die radius is 1 mm (Fig. 6b).

For the identification of differences in damage evolution high strains were targeted to obtain large void area fractions. To achieve high strains without fracture, the specimen were formed at 95 % of the punch displacement at which fracture occurs. The bending radius r_m describes the radius of the neutral fiber. The resulting geometry of the bending specimen consists of a bending angle of 43° with a bending radius of 3.3 mm.

The equivalent plastic strain $\overline{\varepsilon_p}$ in bent parts is

$$\overline{\varepsilon_p} = {}^{2}/_{\sqrt{3}} \bullet \ln\left(1 + {}^{y}/_{r_m}\right) \tag{7}$$

with the coordinate y (distance to neutral fiber) and the bending radius r_m.

Therefore the combined equivalent plastic strain from the pre-strain in tensile tests and the subsequent bending test is calculated to a total of 0.31 (0.22 from bending test) on the outer fibre.

When bending sheets, different stress and strain states exist at the edges and in the internal region. A plane strain state can be assumed for the cross-section orthogonal to the bending axis. A bending test, where the bending stress and the pre-strain are aligned (uni-directional), leads to the strain vector:

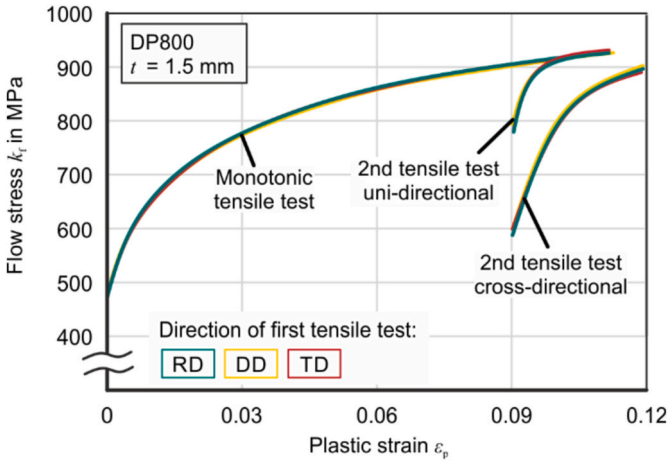

Fig. 9. Flow curves in monotonic tensile test and at uni- and cross-directional load after pre-strain of $\varepsilon_p = 0.09$ parallel and transversal direction at rolling (RD), diagonal (DD) and transversal (TD) direction.

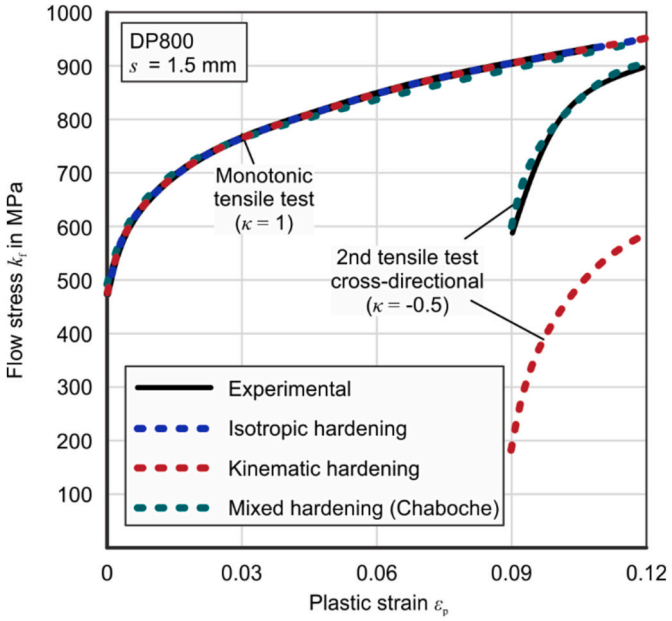

Fig. 10. Flow curves at monotonic loads and after changes of loading direction: experimentally and modelled by isotropic, kinematic and mixed hardening.

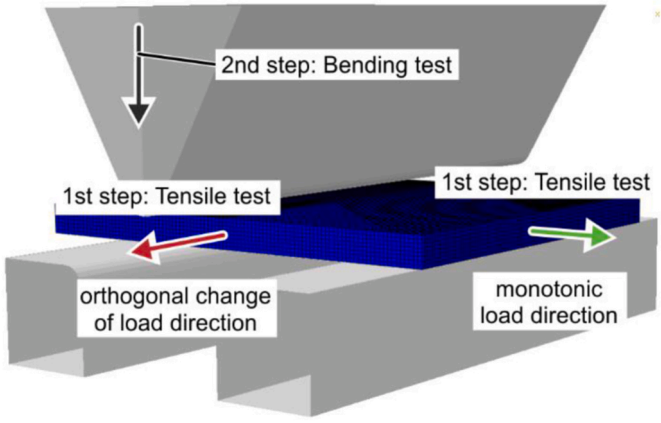

Fig. 11. Numerical setup with constant and orthogonal load directions.

$$d\vec{\varepsilon}_p^{\,2,uni} = \begin{pmatrix} d\varepsilon_p^x \\ d\varepsilon_p^y \\ d\varepsilon_p^z \end{pmatrix} = \begin{pmatrix} d\varepsilon_p^x \\ 0 \\ -d\varepsilon_p^x \end{pmatrix} \tag{8}$$

When the bending stress is oriented orthogonal to the pre-strain (cross-directional), the strain vector is

$$d\vec{\varepsilon}_p^{\,2,cross} = \begin{pmatrix} d\varepsilon_p^x \\ d\varepsilon_p^y \\ d\varepsilon_p^z \end{pmatrix} = \begin{pmatrix} 0 \\ d\varepsilon_p^y \\ -d\varepsilon_p^y \end{pmatrix} \tag{9}$$

According to equation (3), the uni-directional load case is categorized by a monotonic strain path change ($\kappa = 0.87$), while the cross-loading case is categorized by an orthogonal strain path change ($\kappa = 0$).

In bending, the damage evolution mainly occurs on the outer fiber. This can be attributed to the combination of high strains and a positive triaxiality. Therefore, the outer fiber in the cross-section orthogonal to the bending axis is examined for the characterization of damage (Fig. 7). 10 images covering an area of 100 × 100 µm each are acquired per specimen, resulting in an observed area of 0.1 mm^2. The images are captured at the middle of the outer fiber of the bent part. The preparation of specimen and the SEM-parameters are equal to the investigation of tensile specimen in section 2.

When comparing the damage evolution of the specimen, where the loading directions were aligned, the influence of the prior rolling process can be seen (Fig. 8b). The void area fraction was found to be highest at a primary load transversal to the rolling direction (TD), while the lowest damage evolution occurred at a load in diagonal direction (DD). The comparison of DD-specimen shows the effect of a load path change without the influence of the rolling induced microstructure. As in the tensile-tensile sequence, the void area fraction is lower after an orthogonal change of the loading direction. This is also seen for the RD-RD and TD-TD sequence in comparison to the RD-TD and TD-RD sequence. A reason for this can be the void characteristics as described in section 3. When comparing the influence of the load direction change in DD from the tensile-tensile sequence to the tensile-bending sequence, the difference regarding the void area fraction is higher in the tensile-tensile sequence. This might be explained by the influence of anisotropic hardening on the stress state in the tensile-bending sequence, which is investigated in the next section.

4.2. *Influence of load direction changes on anisotropic hardening and its influence on macroscopic stress states*

The tensile-bending sequence is investigated numerically in regards of the stress state in order to find out to what extend the stress state is influenced by anisotropic hardening. Therefore, the material is modelled by isotropic, kinematic and a mixed isotropic-kinematic hardening model.

In the first step, anisotropic hardening in DP800 is identified by the tensile-tensile tests as described in section 2 (Fig. 1). When loaded in the same direction as the pre-straining tensile test, the flow curves show a transition region where the flow stresses are lower than in monotonic tests (Fig. 9). However, after a strain of less than 0.01, the flow stress returns to the same level as in monotonic tests, which can be explained by residual phase stresses (Tarigopula et al., 2008). For cross-directional loading, the initial flow stress is lower compared to uni-directional reloading, and the transition expands over a longer strain region. The stress level approaches the monotonic level, but it cannot be ruled out, based on the conducted experiments, that a permanent softening response may occur. DP800 therefore exhibits a mixed hardening response which can be described by a combined isotropic and kinematic hardening model, e.g. the Chaboche model (Lemaitre and Chaboche, 1990). In regards of different orientations w.r.t. the rolling direction (RD, DD and TD) no differences are to be found in the different testing

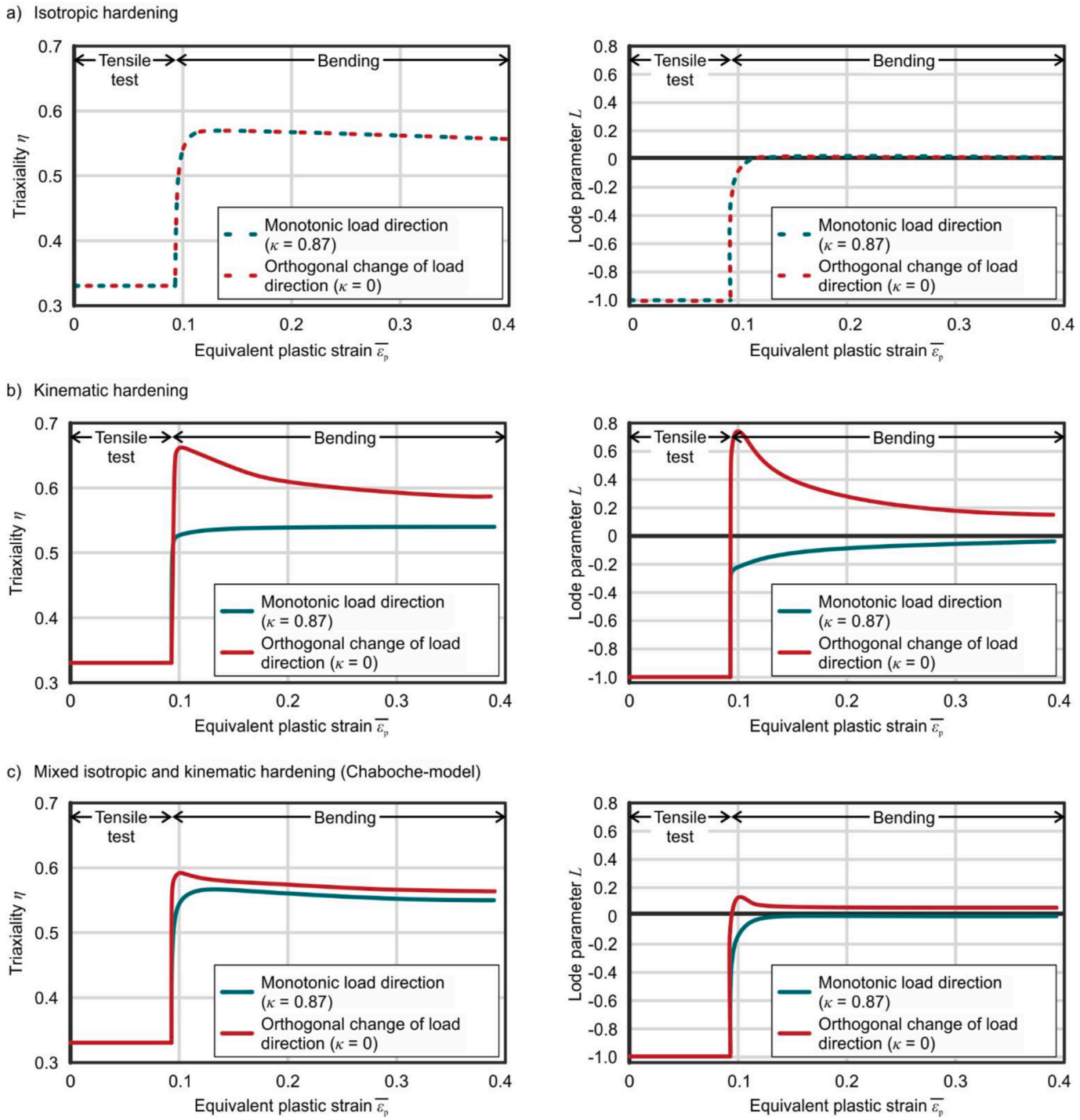

Fig. 12. Triaxiality and Lode parameter in combined tensile and bending test at the outer fiber under a) isotropic, b) kinematic and c) mixed hardening (Chaboche).

sequences.

Purely isotropic and kinematic hardening models are calibrated by the monotonic tensile tests. The Ludwik equation

$$k_f = k_f + C_L \bullet \varepsilon^n \tag{10}$$

is used to identify hardening parameters for the monotonic tensile test (Ludwik, 1909). The parameters are identified in an inverse approach (k_{f0} = 518 MPa, C_L = 955 MPa, n = 0.37), which are the input for the isotropic and kinematic hardening model. To show the influence of a purely kinematic hardening response Zieglers hardening rule (Ziegler, 1959) is used. The kinematic hardening model underestimates the flow stresses after the load direction change heavily (Fig. 10), therefore a mixed isotropic-kinematic hardening model is needed for DP800.

The Chaboche model is used to model the anisotropic hardening response as seen in experiments.

The shift of the yield surface is controlled by the back-stress tensor α which evolves according to

$$\dot{\boldsymbol{\alpha}} = \frac{C \bullet \dot{\overline{\varepsilon}}^p}{\sigma^{f0}} \bullet (\boldsymbol{\sigma} - \boldsymbol{\alpha}) - \gamma \bullet \boldsymbol{\alpha} \bullet \dot{\overline{\varepsilon}}^p, \tag{11}$$

where C and γ denote material parameters that control kinematic hardening and $\boldsymbol{\sigma}^{f0}$ denotes the initial radius of the yield surface.

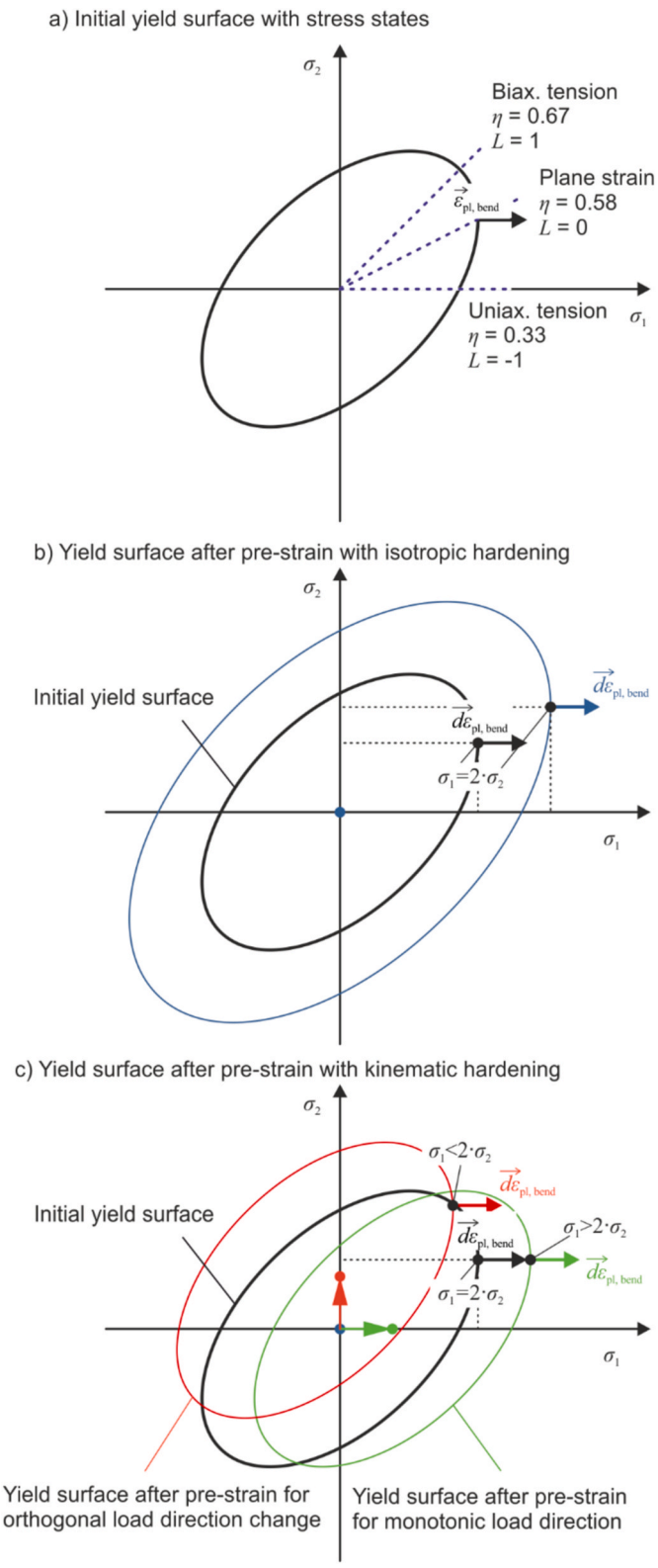

Fig. 13. Development of yield surface and stress states for plane strain condition with isotropic and kinematic hardening models a) Initial yield surface with fundamental stress states, b) Yield surface after pre-strain with isotropic hardening and c) Yield surface after pre-strain with kinematic hardening.

Several backstresses with their corresponding material parameters C_i and γ_i can be used in the model. For the identification of the Chaboche parameters, the hardening in the monotonic tests as well as the anisotropic hardening in the tensile tests at cross directional load are used. The parameters for the Chaboche model are determined by an inverse approach with two backstresses. The identified parameters are: $\sigma_0 =$ 510 MPa, $Q_\infty = 550$, $b = 4$, $C_1 = 21{,}000$, $\gamma_1 = 110$, $C_2 = 300$, $\gamma_2 = 0.1$.

The results of the Chaboche model show good accordance with the experimental results since both the initial flow stress after the load direction change as well as the hardening slope fits well (Fig. 10).

To identify the influence of anisotropic hardening on the stress state during bending after tensile load, a numerical model is set up in Abaqus/Implicit 2019 (Fig. 11).

The Young's modulus is taken as 210 GPa and the Poisson ratio as 0.3 (Hibbitt and Karlsson, 2013). The elements type of the sheet is C3D8R with an element size of 0.2 mm. The tools are analytical rigid shell bodies. The contact properties of the sheet with the punch and the die are modelled by Coulomb friction with a coefficient of 0.1. To simulate the tensile-bending tests, a sheet with dimensions of 50 × 50 × 1.5 mm is strained in one direction up to a plastic strain of 0.09, in accordance with pre-strain in tensile tests, with a release afterwards. In the next step, the punch is moved downwards until released, so that the bending angle of the produced parts is reached. A comparison of the bending region in the numerical setup to the experimental setup exhibits following deviations: bending radius r_m: 3 %, sheet thickness t: +3 %. The triaxiality and Lode parameter during the two forming steps is evaluated for an element on the outer fiber. The influence of the hardening behavior on the stress state in sequences with and without a change of load direction is considered by using isotropic, kinematic and mixed (Chaboche) hardening models separately (Fig. 12).

The stress state during the initial tensile test is the same for all hardening types. Isotropic hardening leads to the same triaxiality and Lode parameter during bending as well, regardless of whether the loading direction is changed or not, whereas for kinematic and mixed hardening models, the stress states differ. After an orthogonal change of loading direction, kinematic hardening leads to an increase in triaxiality (up to 0.66) compared to the load path under isotropic hardening at 0.58, while a monotonic loading direction leads to lower triaxiality (about 0.53). The Lode parameter decreases at a monotonic loading direction to −0.2 and at an orthogonal change of loading direction it increases to 0.7. This trend can also be observed at the simulation with the Chaboche-model, although the differences in the stress state are lower.

This effect can be attributed to the plane strain condition during bending. For a visualization of this effect, a 2D-stress surface is given in Fig. 13, which is justified since σ_3 is 0 in air bending load paths. As for the flow rule after Levy-Mises, the strain increment vector always lies in the exterior normal of the yield surface at the stress point. Since plane strain condition is inevitable in sheet metal bending, the direction of the strain increment is defined and influences the stress state at which plane strain conditions occur when kinematic hardening models are applied.

For isotropic hardening the plane strain condition leads to the mean stress $\sigma_1 = 2 \bullet \sigma_2$. Kinematic hardening on the other hand leads to a translation of the yield surface and therefore changes the ratio between σ_1 and σ_2. For the orthogonal change of loading direction σ_1 decreases while σ_2 increases. This leads to a shift of the stress state into regions with higher triaxiality and Lode parameter. When loaded in the same direction, σ_1 increases while σ_2 decreases. This leads to a shift of the stress state into regions with lower triaxiality and Lode parameter.

High triaxiality and a Lode parameter of 0 leads to higher damage evolution. Hence, regarding the macroscopic stress state, a lower damage evolution would be expected for monotonic loading directions, but experimental results indicate the opposite. This suggests that the influence of the hardening behavior is not the dominant effect for the different damage evolution and fracture. A possible explanation is given by the void evolution after an orthogonal change of loading direction

(Fig. 5): while the void size increases under monotonic loads, an orthogonal change of loading direction leads to a decrease in void size.

When comparing the impact of the loading direction change on damage evolution in the tensile-bending sequences to the tensile-tensile sequences, the difference in tensile-bending sequences was lower than in the tensile-tensile sequences. For this observation, the stress state due to anisotropic hardening could be an explanation.

5. Conclusions

Damage evolution was investigated for tensile-tensile and tensile-bending sequences with varying loading directions on steel grade DP800. Specimens were pre-strained in tensile tests and sub-specimens were loaded by either tensile or bending stresses in the same or in the orthogonal direction regarding the pre-strain. Damage analysis via void area determination by electron microscopy has shown that orthogonal changes of loading direction lead to less damage evolution than monotonic loading directions.

After the pre-straining tensile tests, the orientation of the voids between two martensite phases is mostly transverse to the direction of loading and in between two martensitic phases. Using an illustrative FE-based analysis, it was shown that monotonic loading directions lead to continued growth of these already nucleated voids, while an orthogonal change of loading direction leads to a decrease in void size. This hypothesis of shrinking void area fractions under orthogonal change of loading direction is a possible explanation for the experimental measurements of void area fractions.

The anisotropic hardening behavior of DP800 causes an increase in triaxiality for orthogonal load direction changes in tensile-bending sequences, wherefore, opposed to the experimental results, an increase in void area would be expected. This might also be an explanation for the lower difference in damage evolution in the tensile-bending sequence when compared to the tensile-tensile sequence (DD).

The loading direction w.r.t. the rolling direction has shown to also have an influence on damage evolution, while the initial flow stress and hardening behavior is similar for all directions. Specimens, that were loaded diagonally to the rolling direction revealed the lowest damage evolution, while specimens loaded transversal to rolling direction where most prone to damage evolution.

Future analysis will expand the analysis for arbitrary load direction changes. An RVE will be used to include more detailed aspects regarding damage evolution, such as decohesion and a model-based crack initiation of the martensite phase.

CRediT authorship contribution statement

Philipp Lennemann: Writing – original draft, Investigation. **Yannis P. Korkolis:** Writing – review & editing, Supervision. **A. Erman Tekkaya:** Writing – review & editing, Supervision, Methodology, Conceptualization.

Declaration of competing interest

The authors declare that they have no known competing financial interests or personal relationships that could have appeared to influence the work reported in this paper.

Data availability

Data will be made available on request.

Acknowledgments

The authors kindly thank the German Research Foundation (DFG) for the financial support of project A05 in the Collaborative Research Centre CRC/Transregio 188 “Damage Controlled Forming Processes” (Project number 278868966 – TRR 188). Joshua Grodotzki is acknowledged for the supervision of the research and the review of the paper.

Appendix

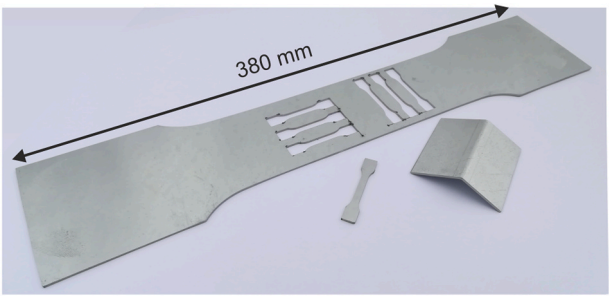

Fig. 14. Specimens.

References

Ahmad, E., Manzoor, T., Ali, K.L., Akhter, J.I., 2000. Effect of microvoid formation on the tensile properties of dual-phase steel. J. Mater. Eng. Perform. 9, 306–310. https://doi.org/10.1361/105994900770345962.

Avramovic-Cingara, G., Ososkov, Y., Jain, M.K., Wilkinson, D.S., 2009. Effect of martensite distribution on damage behaviour in DP600 dual phase steels. Mater. Sci. Eng. 516, 7–16. https://doi.org/10.1016/j.msea.2009.03.055.

Bai, Y., Wierzbicki, T., 2008. A new model of metal plasticity and fracture with pressure and Lode dependence. Int. J. Plast. 24, 1071–1096. https://doi.org/10.1016/j.ijplas.2007.09.004.

Barlat, F., Gracio, J.J., Lee, M.-G., Rauch, E.F., Vincze, G., 2011. An alternative to kinematic hardening in classical plasticity. Int. J. Plast. 27, 1309–1327. https://doi.org/10.1016/j.ijplas.2011.03.003.

Barsoum, I., Faleskog, J., 2007. Rupture mechanisms in combined tension and shear—experiments. Int. J. Solid Struct. 44, 1768–1786. https://doi.org/10.1016/j.ijsolstr.2006.09.031.

Bauschinger, J., 1886. Über die Veränderung der Elasticitätsgrenze und der Festigkeit des Eisens und Stahls durch Strecken und Quetschen und Abkühlen und durch oftmal wiederholte Beanspruchung. Mittheilungen aus dem mechanisch-technischem Laboratorium der K. technischen Hochschule in München 13. Mittheilung XV.

Chaboche, J.L., 1986. Time-independent constitutive theories for cyclic plasticity. Int. J. Plast. 2, 149–188. https://doi.org/10.1016/0749-6419(86)90010-0.

Deng, N., Kuwabara, T., Korkolis, Y.P., 2018. On the non-linear unloading behavior of a biaxially loaded dual-phase steel sheet. Int. J. Mech. Sci. 138–139, 383–397. https://doi.org/10.1016/j.ijmecsci.2018.02.015.

Ha, J., Lee, J., Kim, J.H., Barlat, F., Lee, M.-G., 2014. Meso-scopic analysis of strain path change effect on the hardening behavior of dual-phase steel. steel research int 85, 1047–1057. https://doi.org/10.1002/srin.201300186.

He, X.J., Terao, N., Berghezan, A., 1984. Influence of martensite morphology and its dispersion on mechanical properties and fracture mechanisms of Fe-Mn-C dual phase steels. Met. Sci. 18, 367–373. https://doi.org/10.1179/030634584790419953.
Hibbitt, Karlsson, 2013. ABAQUS Documentation. Dassault Systems, RI, USA.
Kestner, S.C., Koss, D.A., 1987. On the influence of strain-path changes on fracture. Metall. Trans. A 18, 637–639. https://doi.org/10.1007/BF02649479.
Lemaitre, J., Chaboche, J.-L., 1990. Mechanics of Solid Materials. Cambridge University Press.
Lemaitre, J., Dufailly, J., 1987. Damage measurements. Eng. Fract. Mech. 28, 643–661. https://doi.org/10.1016/0013-7944(87)90059-2.
Lode, W., 1926. Versuche über den Einfluß der mittleren Hauptspannung auf das Fließen der Metalle Eisen, Kupfer und Nickel. Zeitschrift für Physik, pp. 913–939.
Ludwik, P., 1909. Elemente der Technologischen Mechanik. Springer Berlin Heidelberg, Berlin, Heidelberg, s.l.
McClintock, F.A., 1968. A criterion for ductile fracture by the growth of holes. J. Appl. Mech. 35, 363–371. https://doi.org/10.1115/1.3601204.
Meya, R., Löbbe, C., Tekkaya, A.E., 2019. Stress state control by a novel bending process and its effect on damage and product performance. J. Manuf. Sci. Eng. 141, 363. https://doi.org/10.1115/1.4044394.
Niazi, M.S., Wisselink, H.H., Meinders, V.T., van den Boogaard, A.H., 2013. Material-induced anisotropic damage in DP600. Int. J. Damage Mech. 22, 1039–1070. https://doi.org/10.1177/1056789512468914.
Prager, W., 1945. Strain hardening under combined stresses. J. Appl. Phys. 16 (12), 837–840.
Pütz, F., Henrich, M., Roth, A., Könemann, M., Münstermann, S., 2020. Reconstruction of microstructural and morphological parameters for RVE simulations with machine learning. Procedia Manuf. 47, 629–635. https://doi.org/10.1016/j.promfg.2020.04.193.
Ramazani, A., Mukherjee, K., Schwedt, A., Goravanchi, P., Prahl, U., Bleck, W., 2013. Quantification of the effect of transformation-induced geometrically necessary dislocations on the flow-curve modelling of dual-phase steels. Int. J. Plast. 43, 128–152. https://doi.org/10.1016/j.ijplas.2012.11.003.
Sampaio, R.F.V., Alexandre, N.S.M., Pragana, J.P.M., Bragança, I.M.F., Silva, C.M.A., Martins, P.A.F., 2023. A software for research and education in ductile damage. Advances in Industrial and Manufacturing Engineering 7, 100127. https://doi.org/10.1016/j.aime.2023.100127.
Tarigopula, V., Hopperstad, O.S., Langseth, M., Clausen, A.H., 2008. Elastic-plastic behaviour of dual-phase, high-strength steel under strain-path changes. Eur. J. Mech. Solid. 27, 764–782. https://doi.org/10.1016/j.euromechsol.2008.01.002.
Voce, E., 1956. A practical strain-hardening function. Metallurg 51, 219–226.
Wierzbicki, T., Xue, L., 2005. On the Effect of the Third Invariant of the Stress Deviator on Ductile Fracture. Impact and Crashworthiness Laboratory, Massachusetts Institute of Technology, Cambridge, MA. Technical report.
Yoshida, F., Uemori, T., 2002. A model of large-strain cyclic plasticity describing the Bauschinger effect and workhardening stagnation. Int. J. Plast. 18, 661–686. https://doi.org/10.1016/S0749-6419(01)00050-X.
Ziegler, H., 1959. A modification of Prager's hardening rule. Q. Appl. Math. 17, 55–65.

Update

Advances in Industrial and Manufacturing Engineering
Volume 9, Issue , November 2024, Page

DOI: https://doi.org/10.1016/j.aime.2024.100147

Advances in Industrial and Manufacturing Engineering 9 (2024) 100147

Contents lists available at ScienceDirect

Advances in Industrial and Manufacturing Engineering

journal homepage: www.sciencedirect.com/journal/advances-in-industrial-and-manufacturing-engineering

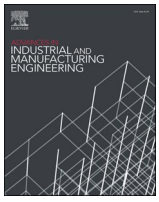

Erratum to "Influence of changing loading directions on damage in sheet metal forming" [Adv. Ind. Manuf. Eng. 8 (2024) 100139]

Philipp Lennemann *, Joshua Grodotzki, Yannis P. Korkolis, A. Erman Tekkaya

Institute of Forming Technology and Lightweight Components (IUL), TU Dortmund University, 44227, Dortmund, Germany

The publisher regrets that the co-author Joshua Grodotzki is missing in the published version.

The publisher would like to apologise for any inconvenience caused.

DOI of original article: https://doi.org/10.1016/j.aime.2024.100139.
* Corresponding author.
E-mail address: Philipp.Lennemann@iul.tu-dortmund.de (P. Lennemann).

https://doi.org/10.1016/j.aime.2024.100147

Available online 23 July 2024